RESEARCH ARTICLE | JUNE 01 1995

Analytical and optimization procedures for determination of all elastic constants of anisotropic solids from group velocity data measured in symmetry planes

Kwang Yul Kim; Rok Sribar; Wolfgang Sachse

Journal of Applied Physics 77, 5589–5600 (1995)
https://doi.org/10.1063/1.359201

Analytical and optimization procedures for determination of all elastic constants of anisotropic solids from group velocity data measured in symmetry planes

Kwang Yul Kim,[a] Rok Sribar,[b] and Wolfgang Sachse
Department of Theoretical and Applied Mechanics, Thurston Hall, Cornell University, Ithaca, New York 14853

(Received 24 October 1994; accepted for publication 9 February 1995)

Analytical and optimization methods of determining all elastic constants of elastically anisotropic solids from the group velocities measured in various directions in the symmetry planes are described. The group velocities in various directions of the specimen are measured, using broadband pointlike and line-type sources in combination with pointlike detectors, and changing a source-to-detector orientation. The mixed index elastic constants of the specimen are determined using analytic formulas that relate the elastic constants to the group velocity in an arbitrary direction on the symmetry plane. It is demonstrated that given the numerous group velocity data, one can efficiently determine the elastic constants by first converting them into phase velocity data and then applying the least-squares optimization methods to the phase velocity data. Examples are provided with specimens of transversely isotropic zinc, cubic silicon, and orthotropic fiber-reinforced poly ether ether kethon. © *1995 American Institute of Physics.*

I. INTRODUCTION

In an elastically anisotropic medium phase and group velocities do not coincide in a general direction of propagation of sound waves. Analytic relations between the elastic constants of elastically anisotropic media and the phase velocities propagating in a general direction in the media are conveniently found in the solution of the Christoffel equation.[1–3] However, no such analytic formula can be easily found in a closed form between a group velocity and elastic constants for an arbitrary propagation direction in an anisotropic medium. Consequently, the elastic constants are most often determined using the measured phase velocity data. The measurement techniques for phase velocities are excellently described in the literature.[4–7] The phase velocities are accurately measured by various ultrasonic plane-wave techniques using either continuous harmonic waves, bursts of harmonic waves, or pulses, which travel through a specimen that has been oriented in a specific direction with two opposite faces polished and parallel to each other. Apart from wave-speed measurements, a resonance technique for a small anisotropic specimen was developed to determine all the elastic constants of a medium.[8,9]

When the destructive sectioning or shaping of a sample is not desired, it is possible to obtain the phase velocities required for complete determination of all the elastic constants. With a rotary composite material specimen immersed in a fluid, Rokhlin and Wang[10] used critical angle measurements for which phase and group velocities coincide. More general considerations between phase and group velocities have been described by Sahay, Kline, and Mignogna.[11] Guided-wave techniques including plate-mode techniques[12] and surface-wave techniques[13] are employed to calculate the elastic constants of a composite specimen, where they are determined by relying on a more complicated numerical method in the absence of closed-form analytic solutions.

Over the last several years some authors[14–19] used a pointlike-source (PS) and pointlike-detector (PD) technique to measure the group velocities. Since a broadband pointlike source generates elastic waves propagating in virtually all directions, this method has advantages that it does not require sectioning or preparation of parallel surfaces of a specimen and at the same time group velocities of both longitudinal L and transverse T modes in many directions of a specimen can be easily obtained by scanning either a source or a detector on the surface of the specimen. The broadband PS-PD technique is applicable even to thick high-loss materials. Group and phase velocities coincide in the principal symmetry directions, along which Aussel and Monchalin[14] measured the group velocities of ultrasound generated by a focused laser beam and detected by a laser interferometer to obtain all three elastic constants of cubic germanium. Doyle and Scala[15] used a laser-line source to determine elastic properties of fiber composites. Their observations relate the elastic constants to bulk waves as well as Raleigh and surface skimming waves. Kim, Sachse, and Every[16–18] used various configurations of pointlike capillary fracture, piezoelectric $Pb(Zr,Ti)O_3$ (PZT), and laser sources in conjunction with a small PZT or capacitive displacement detector to measure the bulk wave group velocities. In a general propagation direction the calculation of group velocities is carried out using a Monte Carlo technique. Niu,[19] for transversely isotropic zinc and fiber-reinforced composite, and Every and Sachse,[20] for cubic media, used the Monte Carlo technique and nonlinear-least-squares iterative method to determine the elastic constants of the materials.

Quite recently, one of the authors[21] derived analytic relations between elastic constants and a group velocity along an arbitrary direction of the symmetry planes of media with

[a]Electronic mail: kykim@msc.cornell.edu
[b]Present address: Engineering Mechanics Laboratory, General Electric Company, P.O. Box 8, Schenectady, NY 12301.

 0021-8979/95/77(11)/5589/12/$6.00

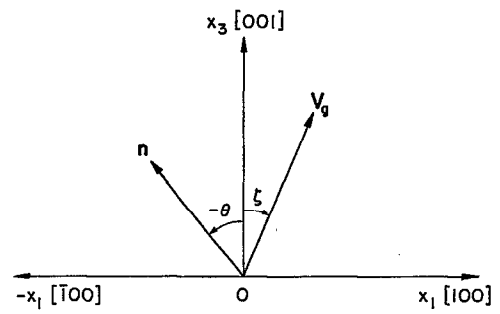

FIG. 1. Coordinate systems for group and phase velocities.

orthorhombic or higher symmetry. In this work, we use these analytic velocity formulas to determine all the elastic constants from the group velocity data measured by PS-PD techniques. In addition, we present a novel method of determining shear horizontal (SH) mode group velocities, which are valuable to determine pure index shear moduli, such as C_{44}, C_{55}, and C_{66}. Furthermore, we propose efficient optimization methods for calculation of the elastic constants by converting the group velocity data into the corresponding phase velocity data. Examples are provided with a thick transversely isotropic zinc disk, a thick cubic silicon disk, and a thin orthotropic fiber-reinforced composite plate. In the former two materials bulk wave group velocities including those of quasilongitudinal (QL), fast transverse (FT), and slow transverse (ST) modes are used for the determination of all the elastic constants, while in the orthotropic composite the group velocities of bulk and surface skimming longitudinal waves are measured for the same purpose.

II. THEORETICAL BACKGROUNDS

Let us denote three principal axes of symmetry of an orthorhombic medium by x_1, x_2, and x_3 directions. Essentially identical relations between the elastic constants and sound wave speed can be found for waves traveling in the three symmetry planes, i.e., x_1x_2, x_2x_3, and x_1x_3, by the proper rotation of indices. Therefore, we take a wave traveling, for example, in the x_1x_3 plane with its wave normal $\mathbf{n}$ and group velocity $\mathbf{V}_g$ oriented at angles θ and ζ, respectively, to the x_3 axis, as depicted in Fig. 1. The positive sense of both θ and ζ is taken in a clockwise direction from the x_3 axis. Because of the reflection symmetry of the x_1x_3 plane across the x_1 axis for media of orthorhombic or higher symmetry, we restrict without loss of generality the range of both ζ and θ to $-90°\leqslant\zeta,\ \theta\leqslant 90°$. Recall that the elastic properties of an orthorhombic medium are characterized with nine elastic constants: C_{11}, C_{22}, C_{33}, C_{44}, C_{55}, C_{66}, C_{12}, C_{13}, and C_{23}.

A. Formulas for the principal symmetry directions

Formulas relating a phase velocity to the elastic constants of solid media are described by many authors.[1–3] Simple relations between the elastic constants and the wave speed exist for waves traveling in the principal symmetry directions, in which the phase and group velocities coincide with each other. The longitudinal L waves traveling with speed V_L along the x_1, x_2, and x_3 directions yield, respectively,

$$\rho V_L^2=C_{11},\quad \rho V_L^2=C_{22},\quad \rho V_L^2=C_{33}. \tag{1}$$

Pure index shear moduli can be calculated from the wave speed of transverse T modes propagating in the principal axis directions. One obtains from the transverse waves propagating with speed V_T along the x_3 direction and polarized in x_1, and x_2 directions, respectively,

$$\rho V_T^2=C_{55},\quad \rho V_T^2=C_{44}. \tag{2}$$

Similarly, C_{44}, C_{55}, C_{66} can be determined from the speeds of pure transverse waves propagating in the x_1 and x_2 directions. Equations (1) and (2) indicate that all pure index elastic moduli can be obtained from the pure L and T waves traveling in the principal symmetry directions of a medium.

B. Phase velocity formulas for the symmetry planes

The pure index shear elastic moduli can be also determined from the pure transverse (PT) modes propagating in an arbitrary direction of the symmetry planes. For example, the following relation holds for the phase velocity of PT mode traveling in the x_1x_3 plane:

$$\rho V_T^2=C_{66}\sin^2\theta+C_{44}\cos^2\theta\quad\text{(PT mode)}. \tag{3}$$

The above equation indicates that both C_{44} and C_{66} can be obtained by measuring PT wave speeds at least in two different directions. By performing similar measurements in the x_1x_2 and x_2x_3 planes all the shear moduli, C_{44}, C_{55}, and C_{66}, can be obtained.

Once the pure index elastic moduli C_{11}, C_{22}, C_{33}, C_{44}, C_{55}, and C_{66} are determined by the method described above, the mixed index elastic moduli C_{12}, C_{23}, and C_{13} can be obtained from the phase velocity measurement of either quasilongitudinal (QL) or quasitransverse (QT) mode propagating in the x_1x_2, x_2x_3, and x_1x_3 planes, respectively. Again, we consider a wave traveling in the x_1x_3 plane. Let us define for simplicity of notation the following identities:

$$\begin{aligned} C_{11\pm}&\equiv C_{11}\pm C_{55},\\ C_{33\pm}&\equiv C_{33}\pm C_{55},\\ C_{13\pm}&\equiv C_{13}\pm C_{55}. \end{aligned} \tag{4}$$

The relations for the QL and QT modes are given by

$$\begin{aligned} 2\rho V_{\mathrm{QL,QT}}^2=&C_{11+}\sin^2\theta+C_{33+}\cos^2\theta\\ &\pm[(C_{11-}\sin^2\theta-C_{33-}\cos^2\theta)^2\\ &+4C_{13+}^2\sin^2\theta\cos^2\theta]^{1/2}, \end{aligned} \tag{5}$$

where the positive and negative signs in front of the square root of Eq. (5) correspond to the QL and QT modes, respectively. Equation (5) relates the elastic constant C_{13} to the phase velocity of QL or QT mode propagating in an arbitrary direction in the x_1x_3 symmetry plane. Suppose that for a

wave normal specified by an angle θ, both QL and QT phase velocities, V_{QL} and V_{QT}, are known for the same angle θ. Then, it follows from Eq. (5) that

$$\rho(V_{QL}^2+V_{QT}^2)=C_{11+}\sin^2\theta+C_{33+}\cos^2\theta$$
$$=C_{33+}+(C_{11+}-C_{33+})\sin^2\theta, \quad (6)$$

$$\rho^2(V_{QL}^2-V_{QT}^2)^2=(C_{11}\sin^2\theta-C_{33-}\cos^2\theta)^2$$
$$+4C_{13+}^2\sin^2\theta\cos^2\theta$$
$$=C_{33-}^2-2(B+C_{33-}^2)\sin^2\theta$$
$$+(C_{11-}^2+2B+C_{33-}^2)\sin^4\theta, \quad (7)$$

where the quantity B is defined as

$$B\equiv C_{11-}C_{33-}-2C_{13+}^2. \quad (8)$$

Similar equations can be found that relate C_{12} and C_{23} to the phase velocity of QL or QT mode propagating in the x_1x_2 and x_2x_3 planes, respectively. Thus, for an orthorhombic medium, all nine elastic constants can be determined from appropriate phase velocity measurements.

C. Group velocity formulas for the symmetry planes

Because of mirror symmetry across the symmetry planes, all the wave normals in the symmetry plane will map themselves onto the corresponding symmetry plane in the group velocity or ray surface. With the exception of a transversely isotropic medium, the converse is not generally true, as is well known in the theory of phonon focusing.[22,23] Because of the nonspherical shape of the QT mode slowness surface of an anisotropic medium, some points with their wave normals that do not lie in the symmetry plane of the QT slowness surface may map themselves into the symmetry plane of the group velocity surface. The group velocity sections that do not correspond to the symmetry plane of the slowness surface are not of our interest here. Again, we consider an elastic wave traveling in the x_1x_3 symmetry plane with its wave normal $\mathbf{n}$ and $\mathbf{V_g}$ at angles θ and ζ measured from the x_3 axis, respectively.

A simple formula that relates group velocity to ζ exists for the PT waves with SH polarization[1,2] and can be expressed as

$$\frac{1}{\rho V_g^2}=\frac{\sin^2\zeta}{C_{66}}+\frac{\cos^2\zeta}{C_{44}} \quad \text{(PT mode)}. \quad (9)$$

Equation (9) indicates that two shear elastic moduli C_{44} and C_{66} can be obtained by measuring the group velocities of PT modes propagating at least in two different directions. By performing similar experiments in the x_1x_2 and x_2x_3 symmetry planes all shear elastic moduli C_{44}, C_{55}, and C_{66} can be determined.

Let us define for simplicity of notation

$$p\equiv\tan\theta, \quad q\equiv\tan\zeta, \quad (10)$$

$$D\equiv[(C_{11-}p^2-C_{33-})^2+4C_{13+}^2p^2]^{1/2}>0. \quad (11)$$

Then it can be shown that B in Eq. (8) and the above D are related by

$$B=\frac{1}{2p^2}(C_{11-}^2p^4+C_{33-}^2-D^2). \quad (12)$$

One of the authors[21] has derived the following Eqs. (13)–(17). The relationship between the directions of group velocity and wave normal is given by

$$q=p\,\frac{B-C_{11-}^2p^2\mp C_{11+}D}{Bp^2-C_{33-}^2\mp C_{33+}D}, \quad (13)$$

which on the substitution of Eq. (12) yields

$$q=\frac{D^2\pm 2C_{11+}Dp^2+C_{11-}^2p^4-C_{33-}^2}{p(D^2\pm 2C_{33+}D-C_{11-}^2p^4+C_{33-}^2)}. \quad (14)$$

We express Eq. (13) in the form of

$$C_{11-}^2p^3+q(Bp^2-C_{33-}^2)-Bp\pm(C_{11+}p-C_{33+}q)D=0. \quad (15)$$

Equation (13) or (15) can be used to find the wave normal corresponding to a given group velocity direction lying in the same corresponding symmetry plane, and vice versa. Equation (14) is quadratic in D, the solution of which as a function of $p=\tan\theta$ is written as

$$D(p)=\frac{1}{1-pq}\{p(\pm C_{33+}q\mp C_{11+}p)\pm[p^2(C_{33+}q$$
$$-C_{11+}p)^2-(1-p^2q^2)(C_{11-}^2p^4-C_{33-}^2)]^{1/2}\}. \quad (16)$$

In the above equation we choose the region of $p=\tan\theta$, where D is real and positive. Finally, the relation for group velocity is given by

$$\rho V_g^2=\frac{(1+q^2)(C_{11-}^2p^4-C_{33-}^2\mp 2C_{33+}D-D^2)^2}{8D^2(C_{11+}p^2+C_{33+}\pm D)}. \quad (17)$$

The upper and lower signs either in $\pm$ or in $\mp$ in Eqs. (13)–(17) apply to the QL and QT modes, respectively, except in the $\pm$ sign in front of the square bracket for square root in Eq. (16), which applies to both QL and QT modes.

Equation (17) expresses the group velocity as a function of $p=\tan\theta$, when D is substituted by the expression on the right-hand side of Eq. (16). Suppose experimentally or by other means as described in Secs. II A and II B that all the quantities including a group velocity V_g, its direction ζ, C_{11+}, C_{11-}, C_{33+}, and C_{33-} are known. Then, Eq. (17) can be solved to find p which makes D in Eq. (16) real and positive. Once the value of this p is found, one can obtain the values of D, B, C_{13+}, and finally C_{13}, using Eqs. (16), (12), (8), and (4), respectively. On the other hand, given the values of all the elastic constants of a medium, Eq. (13) or (15) combined with Eq. (17) can be used to predict the values of QL or QT group velocities in a general direction in the symmetry plane.

For an elastic pulse propagating in the x_1x_2 and x_2x_3 planes, equations equivalent to Eqs. (13)–(17) can be obtained for the QL and QT modes in a similar way by the proper rotation of indices in the notation of the elastic constants. Note that Eqs. (1) and (2) are contained in Eqs. (13)–(17) as a special case, in which $\zeta=\theta=0$ and the phase and

group velocities coincide with each other for both QL and QT modes. Equation (2) is also contained in Eq. (9) as a special case of $\zeta=\theta=0$, in which two transverse modes become degenerate.

D. Extension to higher-symmetry groups

Nine independent elastic constants of an orthorhombic medium are reduced to six for the Laue tetragonal TI group (and also for the TII group when the seventh elastic constant $C_{16}=-C_{26}$ is eliminated by the suitable rotation about the x_3 axis) by the identities

$$C_{11}=C_{22},\quad C_{13}=C_{23},\quad C_{44}=C_{55}, \tag{18}$$

and to three in the cubic symmetry group by the relations

$$C_{11}=C_{22}=C_{33},\quad C_{12}=C_{23}=C_{13},\quad C_{44}=C_{55}=C_{66}. \tag{19}$$

For elastic waves propagating in the x_1x_2, x_2x_3, or x_1x_3 symmetry plane, there is no distinction between the x_1x_3 and x_2x_3 planes for the tetragonal medium and no distinction between all three x_1x_2, x_2x_3, and x_1x_3 planes for a cubic medium. The relations that hold for the symmetry planes of an orthorhombic medium extend to the corresponding symmetry planes of tetragonal symmetry with the substitution of Eqs. (18) into Eqs. (13)–(17) and, likewise, they apply to the cubic symmetry with the substitution of Eq (19) into Eqs. (13)–(17).

Consider elastic pulses of both QL and QT modes traveling in the $\{n_1,n_1,0\}$-type diagonal symmetry planes of tetragonal and cubic symmetry media. The directions of wave normal $\mathbf{n}$ and group velocity are specified by angles θ and ζ to the x_3 axis, respectively. It is shown in Ref. 21 that exactly the same relations between V_g, $\tan\zeta$, $\tan\theta$, and elastic moduli as those found in Eqs. (13)–(17) can be obtained, respectively, by simply replacing C_{11} by K, C_{55} by C_{44}, $C_{11\pm}$ by $K_\pm$. The quantities K, $K_\pm$, and $C_{11\pm}$ are now defined as

$$\begin{aligned} K&\equiv\tfrac{1}{2}(C_{11}+C_{12}+2C_{66}),\\ K_\pm&\equiv K\pm C_{44},\\ C_{11\pm}&\equiv C_{11}\pm C_{44}. \end{aligned} \tag{20}$$

A group velocity formula for a PT wave traveling in the diagonal plane and polarized normal to the plane is found by replacing C_{66} by $(C_{11}-C_{12})/2$ in Eq. (9).

A hexagonal or transversely isotropic medium is characterized by five nonzero elastic constants,

$$C_{11}=C_{22},\quad C_{33},\quad C_{12},\quad C_{13}=C_{23},\quad C_{44}=C_{55}. \tag{21}$$

In addition, the following relation holds for a transversely isotropic medium

$$C_{66}=(C_{11}-C_{12})/2. \tag{22}$$

For a hexagonal or transversely isotropic medium, only the wave normals of both QL and QT modes lying in the symmetry planes map themselves into the corresponding symmetry planes of group velocity surfaces, and vice versa. In addition to the basal symmetry plane, all the planes containing the [0001]-zonal axis are identical symmetry planes.

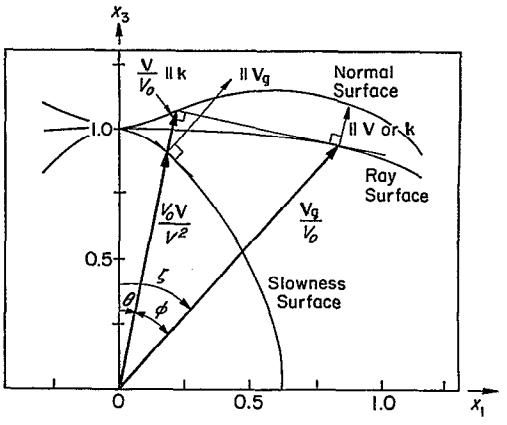

FIG. 2. Diagram relating the surfaces of normalized group and phase velocities, and slowness.

Hence, the formulas developed in orthorhombic and tetragonal media apply unambiguously to a transversely isotropic medium with Eqs. (21) and (22) used for appropriate elastic constants.

E. Conversion between phase and group velocities

The slowness s is defined as an inverse of phase velocity V and expressed as

$$\mathbf{s}\equiv\mathbf{n}/V=\mathbf{k}/\omega, \tag{23}$$

where $\mathbf{k}$ is a wave vector in the same direction as $\mathbf{n}$ and ω denotes the angular frequency. The equations of normal surface N and slowness surface Λ are found from the Christoffel equation. The Christoffel equation and the slowness surface Λ are respectively expressed as

$$\det|C_{ijkl}n_jn_l-\rho V^2\delta_{ik}|=0, \tag{24}$$

$$\Lambda=\det|C_{ijkl}s_js_l-\rho\delta_{ik}|=0. \tag{25}$$

Group velocity $\mathbf{V_g}$ can be obtained from the relation

$$\mathbf{V_g}\equiv\nabla_{\mathbf{k}}\omega=\nabla_{\mathbf{n}}V=\frac{\nabla_s\Lambda}{\mathbf{s}\cdot\nabla_s\Lambda}. \tag{26}$$

The normal surface is the pedal surface of the ray surface and conversely the ray surface is the envelope of planes drawn at right angles to the phase velocity $\mathbf{V}$ on the normal surface.[1,2] These relations are illustrated graphically in Fig. 2, where each surface is drawn using dimensionless phase and group velocities and dimensionless slowness normalized against the corresponding values along the [001] axis in which $\theta=\zeta=0$. These observations can be described by the following relations:

$$\mathbf{V_g}\cdot\delta\mathbf{s}=\mathbf{V_g}\cdot(\delta\mathbf{k}/\omega)=\mathbf{V}\cdot\delta\mathbf{V}_g=\mathbf{n}\cdot\delta\mathbf{V}_g=(\mathbf{k}/\omega)\cdot\delta\mathbf{V}_g=0, \tag{27}$$

$$\mathbf{V}=\mathbf{V_g}\cdot\mathbf{n}. \tag{28}$$

For the phase and group velocities propagating in the symmetry planes, which have been discussed in Secs. II B and II C, Eq. (28) can be written as

$$V=V_g\cos\varphi=V_g\cos(\zeta-\theta), \tag{29}$$

where φ denotes an angle between the directions of a wave normal and the corresponding group velocity. Equations (27) and (28) also hold for the electromagnetic waves.[24]

Given many group velocity data measured along various directions in the symmetry plane, a statistical optimization approach based on a curve fitting to be described next may be more convenient in obtaining elastic constants than the method described in Sec. II C. Equation (27) implies that the direction of a wave normal or a phase velocity points perpendicular to the tangent of a curve that fits the group velocity data, and vice versa given the phase velocity data. These relations are expressed as

$$\tan \varphi = \frac{1}{V}\frac{dV}{d\theta} = \frac{1}{V_g}\frac{dV_g}{d\zeta}. \tag{30}$$

Since we primarily deal with measured group velocity data, we pay attention to the conversion from the group velocity to the corresponding phase velocity data, using the latter part of Eq. (30). Combining Eq. (29) with Eq. (30), one obtains

$$V = \frac{V_g^2}{\sqrt{V_g^2 + (dV_g/d\zeta)^2}}. \tag{31}$$

The dependence of group velocity on a directional angle ζ for a PT mode is given by Eq. (9). The conversion of PT mode group velocities into phase velocities offers no advantage to determination of shear elastic moduli, as can be seen in Eqs. (3) and (9). Since a simple analytical relation between V_g and ζ is not obtainable in a closed form for both QL and QT modes, we choose conveniently to fit group velocity data in a polynomial form as

$$V_g = \sum_{n=0}^{N} c_n \zeta^n, \tag{32}$$

where all the coefficients c_n can be determined by a linear-least-squares method and the constant c_0 represents the group velocity of QL or QT mode along the principal axis for which $\zeta=0$. With these coefficients thus determined, Eqs. (29)–(32) can be used to calculate the phase velocities $V(\theta)$ corresponding to the group velocity data $V_g(\zeta)$. In case that either QL or QT phase velocities $V(\theta)$ can be determined, we fit either of them into Eq. (5) by a nonlinear-least-squares method to obtain relevant elastic constants. On the other hand, when both QL and QT phase velocities can be calculated for the same angle θ, it is much easier to fit both of them into Eqs. (6) and (7) using a much simpler linear-least-squares technique for determination of relevant elastic constants. For plate-shaped composite materials and crystals aligned, e.g., in the x_3 direction normal to the plate, C_{33}, C_{55}, and C_{44} can be easily obtained by measuring L and T wave speeds propagating normal to the plate. Then, one invokes Eq. (6) to find C_{11+}, C_{11}, and C_{11-}. Finally, from Eq. (7) one obtains B, C_{13+}, and C_{13}.

III. EXPERIMENTAL SETUP

Three different kinds of specimens are used to measure group velocities along various directions in the symmetry planes of the specimens: (i) a disk-shaped hexagonal or transversely isotropic zinc crystal that is 25.8 mm thick, 75 mm in diameter, and oriented in the (001) plane; (ii) a disk-shaped cubic silicon that is 49.15 mm thick, 100 mm in diameter, and oriented in the (001) plane; (iii) an orthotropic fiber-reinforced poly ether ether kethon (PEEK) plate that is 190 mm long, 24 mm wide, and 3.26 mm thick with 30% weight fraction of carbon fiber.

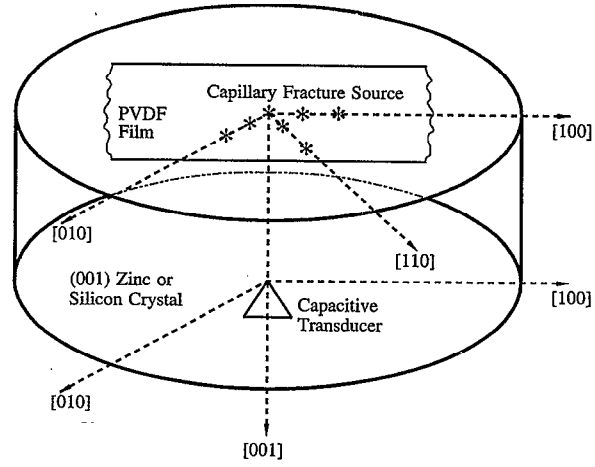

FIG. 3. Geometric schematic of capillary fracture source and capacitive detector used for zinc and silicon specimens.

Four different configurations of ultrasonic source and detector are employed to measure the travel times of various rays that travel at their own distinct group velocities from the source to the detector: first, a capillary fracture source and a capacitive displacement transducer with the round sensing element of diameter 1 mm for zinc and silicon specimens; second, a capillary fracture source and a longitudinal-mode piezoelectric PZT detector of 0.75 mm in diameter for the PEEK specimen; third, a shear-mode PZT source of diameter 0.75 mm and a S PZT detector of the same size for the zinc specimen; fourth, a line-type S PZT source that is 5 mm long and 0.75 mm wide and a S PZT detector of 0.75 mm diameter for the PEEK specimen. A capillary fracture source is activated when a tiny glass capillary of diameter less than 0.1 mm is broken by pressing it vertically on the surface of a specimen with a razor blade. The source-time function associated with the capillary fracture resembles a Heaviside step force with rise time less than 0.1 μs.[25] The former three source-detector configurations correspond to those of a PS and pointlike detector PD and the last configuration may be characterized as that of a line-type source (LS) and PD.

Figure 3 shows a geometric configuration of glass capillary fracture source and capacitive displacement transducer employed with the zinc and silicon specimens. The capacitive transducer senses the displacement component normal to a surface and is fixed at origin on the bottom surface. A 0.08-mm-thick polyvinylidene fluoride (PVDF) film is laid on the top surface of zinc and silicon specimens and the capillaries are broken on the PVDF film at various points lying on the straight line that passes through the epicenter. For the silicon specimen this straight line is parallel to either

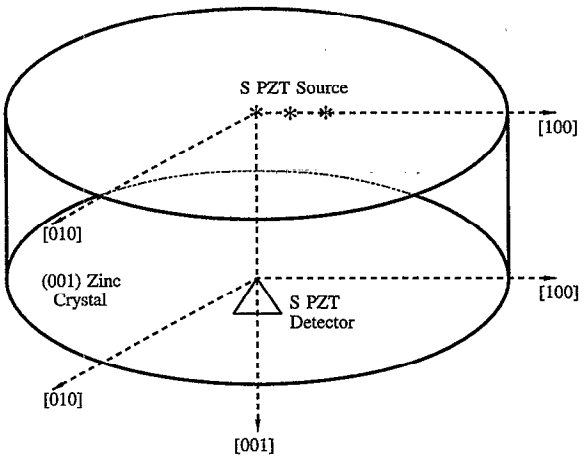

FIG. 4. Geometric schematic of S PZT source and S PZT detector used for a zinc specimen.

the (100), (010), or (110) direction. The elastic waves generated by the capillary fracture at various points on the top surface propagate through the specimen and are detected by the capacitive transducer. The output of the capacitive transducer is amplified by a charge amplifier the bandwidth of which extends from 10 kHz to 10 MHz and the voltage-to-charge sensitivity of which is 0.25 V/pC. The amplified signal is fed into a digitizer which samples it at a 60 MHz rate with 10 bit resolution and the digitized signal is displayed on an x-y scope for visual observation. The output of the PVDF film, generated at the instant of capillary fracture, serves as a trigger to the digitizer and also indicates the time of source excitation that provides a reference time for measurements of travel times of various rays propagating from the source to the detector. All these outputs are stored on the hard disk of a microcomputer for subsequent signal processing and data analysis. The capacitive transducer used in this experiment and its electronic setup are described in detail by Kim *et al.*[26]

Figure 4 displays a geometric schematic of a pointlike S PZT detector with a pointlike S PZT source. This configuration is used for group velocity measurements of SH polarized PT modes with a zinc specimen. The method of measuring the PT mode group velocity by using the PS and PD is described in the article of two of the authors.[17] For measurements of the PT group velocity in a PEEK specimen, the pointlike S PZT source in Fig. 4 is replaced by the LS PZT source. QL mode group velocities of the PEEK specimen are obtained with a capillary fracture source and a L PZT detector that is located on either the top or bottom surface. The source-detector configuration associated with the PEEK specimen is later described in detail in Sec. IV C (see Fig. 9). The S PZT ultrasonic source is excited by a high-voltage pulse derived from the Panametrics model 5055PR. The signals detected by the L- or S-mode PZT transducers are amplified with 40 or 60 dB gain by a low-noise amplifier, the bandwidth of which extends from 20 kHz to 2 MHz. The amplified signals are brought into a digitizer with a 60 MHz sampling rate, fed into an x-y scope, and, finally, stored in a microcomputer.

A major measurement error of about 1% in group velocities of zinc and silicon is due to a finite size of the detector (0.75 or 1 mm in diameter) located in nonsymmetry directions. Along the epicentral symmetry directions of these specimens the variation of group velocity with source-to-detector orientation is zero to first order and a major error as large as 0.2% in group velocity data derives from the finite sampling rate and bandwidth of system. The overall error is estimated to be about 0.4% in pure index elastic moduli C_{ij} $(i=j)$ and about 5% in mixed elastic constants C_{ij} $(i\neq j)$ both for zinc and for silicon. A major error in group measurement of the PEEK specimen is overshadowed by the variation of group velocity due to inhomogeneity of the material and described in Sec. IV C.

IV. DETERMINATION OF ELASTIC CONSTANTS

A. Transversely isotropic zinc

Two of the authors[27] determined five elastic constants of hexagonal zinc accurately from the group velocity data measured in two principal directions. They are listed in Table I. For zinc we simplify the four index notations [0001] and

TABLE I. The elastic constants of zinc obtained by various methods in units of GPa.

Method No.	Method used	Equation used	Elastic constant (GPa)				
			C_{11}	C_{33}	C_{44}	C_{12}	C_{13}
1	Ref. 27	Eqs. (1), (2), (34)	163.75	62.93	38.68	36.28	52.48
2	L and T V_g in two principal directions and OL V_g at $\zeta=47.3°$	Eqs. (1), (2), (16), (17)	...	...	...	...	52.5
3	L and T V_g in two principal directions and IQT V_g at $\zeta=11.0°$	Eqs. (1), (2), (16), (17)	...	...	...	...	51.3
4	L and T V_g in two principal directions and SQT V_g at $\zeta=11.0°$	Eqs. (1), (2), (16), (17)	...	...	...	...	53.3
5	QL and PT V_g in the symmetry plane and nonlinear-least-squares fit	Eqs. (2), (5), (9) Eqs. (30)–(33)	163.7	62.6	38.8	37.3	52.4
6	QL, QT, and PT V_g in the symmetry plane and linear-least-squares fit	Eqs. (6), (7), (9) Eqs. (30)–(33)	164.1	62.6	38.8	37.3	52.2

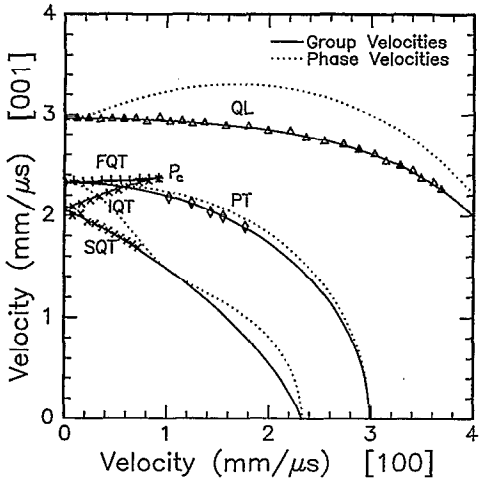

FIG. 5. The (010) section of group and phase velocity surfaces in zinc, where the measured group velocity data are juxtaposed.

(0001) used for a hexagonal crystal to [001] and (001), respectively, which are appropriate for transversely isotropic media including fiber-reinforced composite materials. Using the elastic constants of Ref. 27 and Eqs. (9), (15), and (17) corresponding to a hexagonal medium, the group velocities of PT, QL, and QT modes propagating in various directions are calculated and the (010) section of these group velocity surfaces is drawn with solid lines in Fig. 5, which also shows for comparison the same section of phase velocity surfaces drawn with dotted lines. The phase velocities of various modes are calculated using Eqs. (3) and (5). The measured group velocity data, which were obtained with the configurations shown in Figs. 3 and 4 and are described in detail in Ref. 17, are juxtaposed for comparison in Fig. 5. The directional range ζ of the measured group velocities is within 58° for the QL mode, 45° for the PT mode, and 25° for the QT mode. For group velocity directions ζ larger than 25° lying outside the cuspidal region, a QL mode reflected from the side walls of the finite-sized zinc specimen arrives ahead of the slow QT (SQT) ray, smearing the arrival of the SQT ray in the detected signal and making an accurate determination of the SQT group velocity very difficult.

The (010) section is a typical representation of the zonal planes belonging to the [001] zone in zinc and [001] is the symmetry direction in zinc. In Fig. 5, QL, FQT, IQT, and SQT stand for the quasilongitudinal, fast quasi-transverse, intermediate (speed) quasitransverse, and slow quasitransverse, respectively. These modes are all polarized in a sagittal plane coinciding with the [001] zonal plane. The PT denotes a pure transverse mode, which is SH polarized normal to the zonal plane and parallel to the (001) basal plane. Using the analytical formulas found in Ref. 21, the direction of the cuspidal edge P_c shown in Fig. 5 is calculated to be 21.54° from the [001] direction.

1. Determination of mixed index elastic constant

Experimental determination of all the elastic constants including the mixed index elastic constants C_{12} and C_{13} by the measurement of phase velocities is excellently described in Refs. 4 and 5. Using Eqs. (16) and (17) derived for both QL and QT modes, we now demonstrate how the mixed index elastic constant C_{13} can be determined from the group velocity data measured along an arbitrary direction in the zonal plane. The values of four elastic constants, C_{11} =163.75 GPa, C_{33}=62.93 GPa, C_{44}=38.68 GPa, C_{12}=36.28 GPa, identical to those of Ref. 27 listed in Table I, are obtained from the group velocity data of pure longitudinal and pure transverse modes measured in two principal directions by using the expressions corresponding to Eqs. (1) and (2) for a hexagonal medium and relation (22). We take first the QL group velocity V_g=3.910 mm/μs measured in the direction of ζ=47.3° outside the cuspidal region shown in Fig. 5. Simultaneous equations of Eq. (16) with the negative square root and Eq. (17) are applied to the QL mode to solve for p=tan θ and D. They yield no real solution for p; however, Eqs. (17) and (16) with the positive square root yield θ=17.7°, D=59.4 GPa, and C_{13}=52.5 GPa in excellent agreement with the C_{13}=52.48 GPa of Ref. 27 listed in Table I. Next, we take the IQT mode group velocity V_g=2.293 mm/μs measured in the direction ζ=11.0° inside the cuspidal region. Equation (16) with the positive square root and Eq. (17) for the QT mode yield two solutions: θ=11.1°, D=37.9 GPa, and C_{13}=37.9 GPa; θ=−18.9°, D=62.2 GPa, and C_{13}=51.3 GPa. As indicated in Fig. 2 and also by Eq. (27), the direction of the wave normal θ at the point of a group velocity surface is in the direction of the outward gradient at that point, which for the IQT branch in Fig. 5 points in the negative direction (or to the left-hand side) from the [001] direction. The former set of values for the positive θ is therefore discarded. The latter value 51.3 GPa of C_{13} compares well with the above-quoted value 52.48 GPa within 3% error. The values of C_{13} obtained from the QL group velocity at ζ=47.3° and the IQT group velocity at ζ=11.0° are, respectively, listed in the no. 2 and 3 rows of Table I for comparison. Similarly, using the measured SQT group velocity 1.899 mm/μs at ζ=11.0°, one obtains C_{13}=53.3 GPa, which is listed in the no. 4 row of Table I and falls within 1.6% from the C_{13} value of Ref. 27. The QL and FQT group velocities obtained near the symmetry direction [001] are not recommended for determination of C_{13}, unless they are very accurately measured, say, with an error of about 0.01%. For these QL and FQT modes, the directions of the corresponding wave normals are also close to the symmetry direction. For small values of θ, $\partial C_{13}/\partial V_g$ is large and a small error in group velocity measurement results in a large error in the C_{13} value.

The mixed index elastic constant C_{12} can be also determined from the PT mode group velocity, e.g., V_g=2.523 mm/μs measured in the direction of ζ=37.9° outside the cuspidal region, using Eqs. (9) and (22). C_{44}=38.68 GPa, which was determined from the PT wave group velocity propagating in the [001] direction and is identical to the C_{44} value of Ref. 27, is used in Eq. (9) to obtain C_{12}=36.3 GPa in excellent agreement with the C_{12}=36.28 GPa listed in Table I. The latter value of C_{12} was obtained from the PT group velocity propagating in the basal plane.

The determination of C_{12} or C_{66} from the group velocity of a SH polarized PT mode propagating in an arbitrary di-

rection in the zonal plane requires more substantial explanation. As mentioned in Sec. II and described in detail in Ref. 17, the SH polarized group velocities have been measured by using the S PZT source and S PZT detector, which were both polarized in the same direction and situated on the opposite faces of a specimen. The S PZT source can be modeled as a monopolar source acting in a horizontal direction, for example, the direction 1 representing the [100] on the surface. Any direction on the top surface plane (001) is identical to the [100] in a transversely isotropic zinc. With a Heaviside step source acting at origin, the SH polarized PT mode displacement response, $\tilde{G}_{11}(\mathbf{x},t)$, as a function of the detector position $\mathbf{x}$ and time t, is described by Every and Kim.[28] The SH motion caused by the QL mode arrival is a near-field effect, diminishing with the inverse square of the distance r from a source to a detector and, consequently, it is difficult to observe in a far field. r in our experiment is much larger than the dominant wavelength of the signal and therefore belongs to the far field. Indeed, it is observed that the SH motion caused by the QL mode arrival, being followed by a shallow and slowly changing slope in the displacement curve, is too weak to be detected by the pointlike S PZT detector located in the far field, which detects only the arrivals of various QT and PT modes. Within and without the cuspidal region the first arrivals detected by the S PZT detector are associated with the FQT and PT modes, respectively. The group velocities obtained with these first arrivals outside the cuspidal region are plotted with diamond symbols in Fig. 5 and they fit well the theoretical PT curve calculated using Eq. (9). Recall that the SH mode group velocity measured at $\zeta=37.9°$ has been previously used to obtain the value of C_{12}.

2. Determination of elastic constants by statistical optimization

Even though the measurements in different principal directions yield the most accurate determination of elastic constants, there may arise a situation in which faceting of a sample is not desired and therefore the group velocity of some mode, say QT, can be measured in only one principal direction. Such is often the case in the nondestructive testing of a composite plate, where QL and QT mode group velocities in many different directions are obtained by scanning the top surface preferably in the principal-axis direction. Suppose now that pure longitudinal and transverse wave speeds in a direction on the basal plane of zinc cannot be obtained and consequently the values of the elastic constants C_{11} and C_{12} are not directly available. What we have on hand is the group velocity data shown in Fig. 5, which have been obtained by scanning the top surface of a (001)-oriented zinc specimen along the straight line passing through epicenter. Given these group velocity data, is it possible to determine all five elastic constants of zinc? The answer is definitely yes and next we show how they can be uniquely determined.

First, both C_{33} and C_{44} can be determined from the group velocities of pure L and T modes propagating along the symmetry direction [001]. Then using the value of C_{44} and Eq. (9), C_{12} can be determined from the PT mode group velocity data shown in Fig. 5, as discussed in the previous subsection. Finally, both C_{11} and C_{13} can be determined through Eqs. (16) and (17) choosing any combination of two among the QL and QT group velocity pairs in the same or a different direction and among the two QL or two QT velocities in different directions. This last analytical approach is considerably complicated and sometimes unwieldy. Given many group velocity data in various directions, one may even try a nonlinear-least-squares goodness fit to Eqs. (16) and (17) for determination of either all five elastic constants or just two elastic constants of C_{11} and C_{13}. The nonlinear-linear-squares method depends on good initial estimates of parameters, the convergence of which to the optimal value is not always guaranteed.

The difficulties arising in the above situation can be circumvented by using the statistical optimization technique described in Sec. II E. The elastic constants can be obtained more conveniently and efficiently through the statistical approach. The accurate conversion of group velocity data into the corresponding phase velocity data is most essential for successful implementation of this method. Equations (30) and (31) indicate that the accurate conversion depends not only on the accurate value of group velocity but also on its derivative with respect to its directional angle ζ as well. This means that a polynomial form we choose for fitting the QL and various QT branches should fit the data very well not only globally but also locally. The group velocity curve changes both its slope and curvature continuously in the whole range $-90°\leqslant\zeta\leqslant 90°$, as can be seen in Fig. 5. Polynomials of degree equal to or more than 4 are found to work very well for zinc. For simplicity and convenience we choose a polynomial of degree 4 ($N=4$) in Eq. (32) to fit the group velocity data. For a group velocity data curve that changes its curvature appreciably in the entire experimental ζ range, a polynomial of degree higher than 4 may be preferred. For the PT group velocity data a polynomial fitting is not necessary, as explained in Sec. II E and, instead, Eq. (9) is used to fit the PT data outside the cuspidal region in Fig. 5. Note that because of mirror symmetry across the symmetry axis [001], the IQT and SQT branches are in fact one smoothly joining branch, when their reflected mirror images are extended across the symmetry axis. The QL, FQT, and IQT-SQT group velocity data are fitted into the polynomial of degree 4 to determine its coefficients by a linear-least-squares method.

The constant coefficients c_0 associated with the QL and FQT branches and determined by the curve fitting are related to the elastic constants by

$$\rho(c_0^2)_{\mathrm{QL}}=C_{33}, \quad \rho(c_0^2)_{\mathrm{FQT}}=C_{44}. \tag{33}$$

Once all the polynomial coefficients are determined, the elastic constants C_{33} and C_{44} are obtained according to Eq. (33). Then, one obtains the quantities $C_{33\pm}=C_{33}\pm C_{44}$ and the phase velocities $V(\theta)$ of QL and QT modes using Eqs. (29)–(31). Next, the quantities on the left-hand side of Eqs. (6) and (7) versus $\sin^2\theta$ are calculated and they are fitted into these equations by the linear-least-squares method to determine $C_{11+}=C_{11}+C_{44}$, $C_{13+}=C_{13}+C_{44}$, C_{11}, and C_{13}. Figure 6 shows that the calculated data $\rho(V_{\mathrm{QL}}^2+V_{\mathrm{QT}}^2)$, plotted versus $\sin^2\theta$, lie closely to the straight line, the slope of which equals $C_{11+}-C_{33+}$, as Eq. (6) indicates. Because of

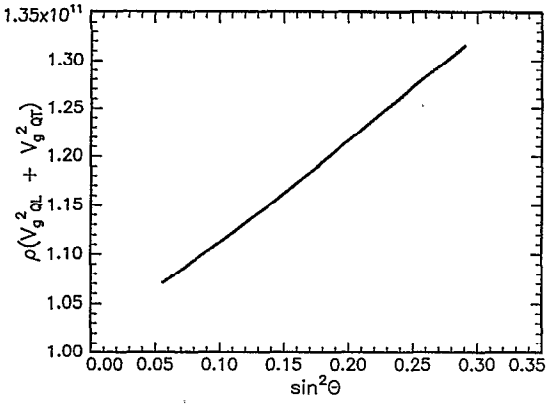

FIG. 6. $\rho(V_{QL}^2+V_{QT}^2)$ vs $\sin^2\theta$ calculated from the group velocity data. The ordinate is in units of kg/(m s^2).

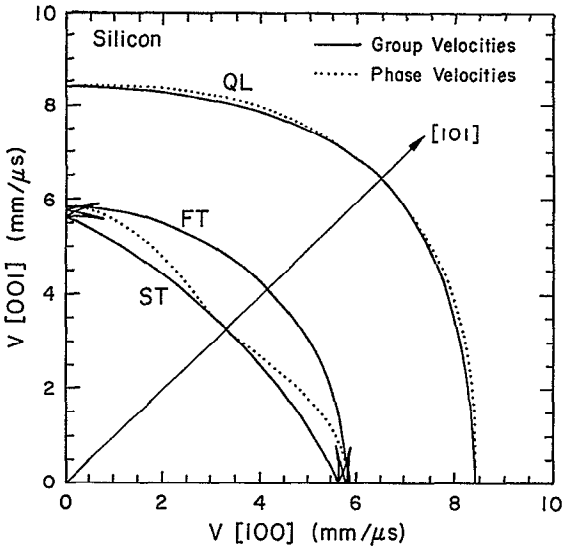

FIG. 7. The (010) section of the group and phase velocity surfaces in silicon.

rather complex mapping between the directions of group velocity and wave normal, the converted QL and QT phase velocities lie in the θ range less than 35°. Using the value of C_{44} found above and Eq. (22), C_{12} is obtained from the PT group velocity data by the linear-least-square fit into Eq. (9). All five elastic constants of zinc thus determined by the statistical optimization technique are listed in the no. 6 row of Table I and compare very well with those of Ref. 27 in the same table.

Kim and Sachse[27] derived an analytic equation that relates $C_{13+}=C_{13}+C_{44}$ to the constant coefficient c_0 obtained from the curve fitting of the IQT and SQT group velocity data and it is expressed as

$$(C_{13}+C_{44})^2=C_{11}C_{33}+C_{44}^2-\rho c_0^2(C_{11}+C_{44}) +2[C_{11}C_{44}(C_{33}-\rho c_0^2)(C_{44}-\rho c_0^2)]^{1/2}. \tag{34}$$

The coefficient c_0 obtained from the group velocity data of the IQT-SQT branch is 2.051 mm/μs. Using the values of C_{33}, C_{44} and C_{11} obtained from the curve fitting and Eqs. (33) and (6), one obtains from Eq. (34) C_{13}=52.8 GPa, which is in excellent agreement with C_{13} of Ref. 27. A similar equation to Eq. (34), obtained by interchanging indices 1 and 3, applies to transversely isotropic media that have a cusp of the QT mode around the basal plane.

B. Cubic silicon

A majority of crystals found in nature is solidified in a cubic crystal form. Here we illustrate a determination of the elastic constant C_{12} of cubic silicon using Eqs. (16) and (17) adapted to a cubic medium and a QL mode group velocity measured in a direction lying in the (010) plane. For $\zeta=0$ that corresponds to $\theta=0$, Eqs. (15) and (17) together with the relation (19) yield $\rho V_g^2=C_{11}$ and $\rho V_g^2=C_{44}$ for the pure L and T modes propagating along the ⟨100⟩ direction, respectively. Similarly, in Eqs. (15) and (17), we replace C_{11} by K in Eq. (20) and $C_{11\pm}$ by $K_\pm$ in Eq. (20) and use for $\zeta=90°$ relation (19) to find the following relations: $\rho V_g^2=K=(C_{11}+C_{12}+2C_{44})/2$ for the pure L mode and $\rho V_g^2=(C_{11}-C_{12})/2$ for the PT mode propagating in the [110] direction. The same relations in the ⟨110⟩ direction can be obtained for $\zeta=45°$ using Eqs. (15) and (17) and relation (19). The values of elastic constants C_{11}=165.7 GPa and C_{44}=79.56 GPa are obtained from the pure L and pure T group velocity data measured in the [001] direction and the density of 2332 kg/m^3. Another independent measurement of pure L and pure T modes propagating in the [110] direction yields C_{12}=63.90 GPa. Using these values of elastic constants, the Monte Carlo generated (010) section of group velocity surfaces is plotted in Fig. 7, which also shows the phase velocities for comparison. It displays very complex folded features of the QT mode group velocity sheet around the cubic axis. The QT group velocity sheet in Fig. 7 consists of that of the slow transverse (ST) modes that are sagittally polarized and that of the fast transverse (FT) modes that are perfectly SH and nearly SH polarized. An enlarged view (not shown here) of the QT folded sheet manifests one cusp arising due to the wave normals lying in the (010) plane and the other three foldings due to the wave normals oriented in the nonsymmetry planes.[16]

The QL group velocity 8.83 mm/μs is determined from the QL mode arrival indicated in the signal shown in Fig. 8, which is detected by a miniature capacitive transducer located at a distance of 25 mm (ζ=26.9°) from epicenter in the [100] direction on the bottom surface of a (001) silicon specimen. A broadband ultrasonic wave is generated by a capillary fracture source located at origin on the top face. We use D with a positive square root in Eq. (16) and Eq. (17), together with relation (19) for a cubic medium, C_{11}=165.7 GPa, C_{44}=79.56 GPa, V_g=8.83 mm/μs, and ρ=2332 kg/m^3, to obtain only one real value of C_{12}=64.4 GPa, which is in good agreement with the C_{12}=63.9 GPa mentioned above. D with a negative square root in Eq. (16) and Eq. (17) has no real root for $p=\tan\theta$. Using C_{12}=63.9 GPa with the same values of C_{11} and C_{44} as above in Eqs. (15) and (17) predicts

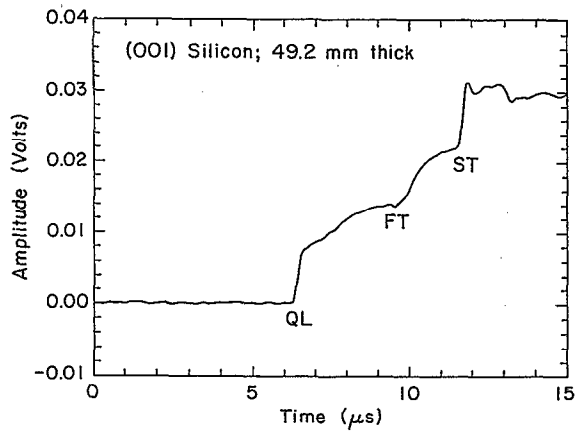

FIG. 8. A displacement signal detected by the capacitive transducer at a distance of 25 mm from epicenter in the [100] direction on the bottom surface.

the QL group velocity equal to 8.827 mm/μs in the direction of the detector. Note that an error as small as 0.032% in group velocity measurement results in an error as large as 0.79% in the elastic constant C_{12}. Using the arrival of the slow QT mode marked as ST in Fig. 8 with Eqs. (16) and (17) leads to a similar result. A small dimple found around 9.5 μs in the signal is caused by the arrival of nearly SH polarized FT modes which travel at a group velocity indistinguishably close to $(C_{44}/\rho)^{1/2}$. Note that using the arrivals of QL, FT and ST modes in one directional signal, it is possible to determine all three elastic constants of cubic silicon. It is shown by Kim, Every, and Sachse[21,29] that all three elastic constants of a cubic medium can also be determined from the L or QL group velocities measured in three different directions lying in the symmetry planes and that all three elastic constants of silicon can be easily and accurately determined from one broadband signal propagating in the ⟨100⟩ direction.

C. Orthotropic fiber-reinforced plate of PEEK

A carbon-fiber-reinforced PEEK plate specimen shown in Fig. 9 has the density of 1500 kg/m^3. Recall that phase and group velocities coincide along the principal symmetry directions and they have extremal values along these directions. Note also that QL, QT, and SH polarized PT modes exhibit a mirror symmetry across the symmetry planes. Using these properties of the group velocity patterns obtained for various source-to-detector orientations, it is observed that the PEEK specimen possesses orthotropic symmetry for which the x_1, x_2, and x_3 directions shown in Fig. 9 are those of three principal axes. It has the maximum and minimum longitudinal wave speeds along the x_1 and x_3 directions, respectively.

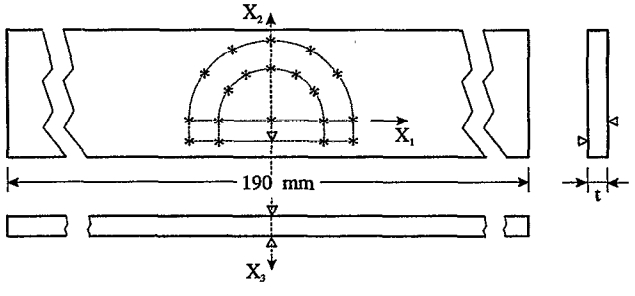

* Capillary Fracture or S PZT Source; ▽ L or S PZT Detector

FIG. 9. Material coordinate axes and various configurations of the detector and scanning sources used for a PEEK plate.

With the specimen anisotropy determined as above, we are now at the stage of finding all the nine elastic constants of the orthotropic specimen. The several L group velocities along the x_3 direction are measured by breaking the glass capillary on many different spots of the top surface and placing the L PZT detector at epicenter on the bottom face. About several percent nominal variation in the wave speeds is observed because of inhomogeneity of the material. The average value of the wave speeds is used to calculate the elastic constant C_{33}=10.7 GPa, according to Eq. (1). Similarly, with the L PZT detector at origin on the top surface, C_{11}=28.5 GPa and C_{22}=15.2 GPa are obtained from the average of the pseudo-L wave speeds in the x_1 and x_2 directions, respectively. These L waves are launched from the capillary fracture sources scanned in the x_1 and x_2 directions on the top surface. Since the arrival time of the L or QL modes generated by the capillary fractures is unambiguously identified as the first arrival of the signal, we omit a display of the signal here.

The pure index elastic constants C_{44} and C_{55} can be determined by transmitting the plane waves of transverse mode along the x_3 direction, which are polarized in the x_2 and x_1 directions, respectively, and by measuring their wave speeds. These plane-wave modes are not used in this experiment. Instead, we determine the pair of C_{44} and C_{66} values and the pair of C_{55} and C_{66} values by fitting the SH polarized PT group velocities obtained in the x_1x_3 and x_2x_3 planes into a form of Eq. (9). A pointlike S mode PZT detector with a sensing element of diameter 0.75 mm is positioned at origin on the bottom face. First, a line-type S mode PZT source with an activation area that is 5 mm long and 0.75 mm wide and polarized in the long 5 mm direction, is scanned along the x_1 direction across the epicenter on top surface in the x_1 range from 0 to 7.5 mm. The choice of the LS PZT source, in lieu of a PS PZT source, is simply a matter of convenience in identifying the PT mode arrival by enhancing the ratio of SH motion associated with the PT arrival to that associated with the arrivals of other modes polarized in the sagittal plane. The source polarization is always maintained in the x_2 direction. Because of a relatively thin sample thickness of 3.26 mm, the detector positions correspond to a near field and thereby a SH motion ensuing the first arrival of the QL mode is observed in the detected signal, in contrast to the corresponding case in zinc discussed in Sec. III A, where the detector is positioned in the far field and the QL mode arrival is undetectable. However, the first large amplitude in the detected signal is found following the arrival of the PT mode that is SH polarized normal to the sagittal plane. A typical

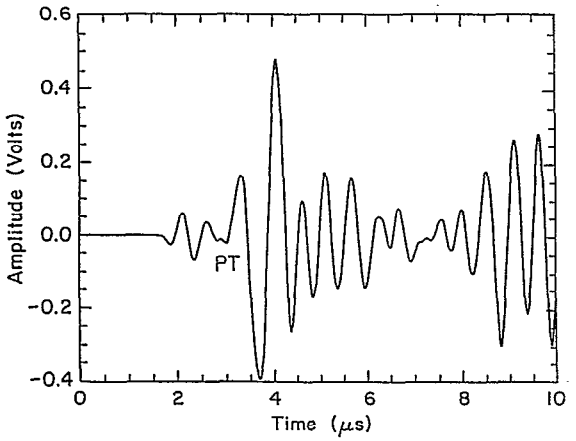

FIG. 10. A typical off-epicentral SH signal detected by the S PZT transducer located in the x_2x_3 plane with a LS PZT source. Both source and detector are polarized in the x_1 direction.

wave form recorded is displayed in Fig. 10, where PT indicates its arrival time. Detailed description of the PT arrival is given elsewhere.[28,30] The group velocities obtained for various source locations are fitted into Eq. (9) to obtain the values of C_{44} and C_{66}. Similarly, the values of C_{55} and C_{66} are obtained with the LS polarized in the x_1 direction and scanned in the x_2 direction across the epicenter. The obtained average values of the pure index elastic constants are C_{44} =2.23 GPa, C_{55}=2.41 GPa, and C_{66}=5.71 GPa with several percent standard deviation.

The mixed index elastic constant is calculated from the QL group velocity data obtained along arbitrary directions in the principal planes, using Eqs. (16) and (17). The capillary fracture source and L mode PZT detector are used for this purpose. The average of several C_{12} values, 7.70 GPa, is obtained from the pseudo-L wave group velocity data in various directions with both source and detector located on the top surface. The averaged C_{13} value equal to 6.00 GPa is obtained from the QL group velocity data measured along several different directions in the x_1x_3 plane with the source and detector located on the top and bottom sides, respectively. Finally, the averaged C_{23} value equal to 7.65 GPa is obtained with the source and detector located in the x_2x_3 plane on the opposite sides of the specimen. The nine elastic constants of the carbon fiber PEEK specimen are listed in Table II.

The calculated Young's modulus in the x_1 direction, obtained using the above elastic constants of the PEEK specimen, is 24.0 GPa, which compares well with the Young's modulus 23.0 GPa obtained by the static tension test performed in the same direction.

TABLE II. The elastic constants of the orthotropic PEEK plate in units of GPa.

C_{11}	C_{22}	C_{33}	C_{44}	C_{55}	C_{66}	C_{12}	C_{13}	C_{23}
28.5	15.2	10.7	2.23	2.41	5.71	7.70	6.00	7.65

The specimen material is not uniformly homogeneous everywhere and anisotropy varies slightly from point to point from the overall orthotropic symmetry. Moreover, because of the relatively thin sample thickness, the small aperture source and detector are not exactly pointlike. Therefore, the variations in the obtained elastic constants are much larger, particularly in the mixed index elastic constants that show the variations as large as 20% from the average value, as compared with those of zinc and silicon crystalline specimens,. The method of using small sized source and detector is not particularly well suited for measurement of all the elastic constants of a thin plate specimen. Here we have merely shown an analytical methodology for determination of all the elastic constants of an orthotropic plate.

V. DISCUSSION

Pure index L moduli, such as C_{11}, C_{22}, and C_{33}, are most easily obtained with least errors, from the L group velocities, because their arrival in the detected signal is unambiguously found at the point from which the signal jumps from the noise level. For the same reason, the pure index shear moduli, such as C_{44}, C_{55}, and C_{66}, can be easily determined for a thick specimen oriented in the principal plane, where a detector can be located in the far field. Care should be taken to avoid a propagation direction inside the cuspidal region, because the first arrival in the signal detected only outside the cuspidal region corresponds to the SH polarized PT mode. For a relatively thin specimen the PT arrival can be determined with a modicum difficulty, as discussed in Sec. IV C with a PEEK specimen.

The QL and QT modes are coupled in a broadband signal and they are polarized mutually perpendicular to each other in the same sagittal plane. For determination of mixed index elastic constants, such as C_{12}, C_{23}, and C_{13}, it is highly recommended to choose the arrival times of the QL mode for its easy, unambiguous identification. Except for the displacement signal detected by the displacement transducer such as a capacitive transducer, the unambiguous identification of the QT mode arrival is generally quite difficult in a broadband signal detected by a thin disk-shaped PZT, partly because of the effect of lingering QL mode and in some directions a head wave superposed on the QT mode and partly because of the ringing of the detecting transducer. There is another reason why the QL group velocity is preferred: There is no folding of the QL ray surface where the cusp is absent in all directions, because the corresponding QL slowness surface is everywhere convex for all media.[31] All the points on the symmetry plane of the QL slowness surface map into the corresponding symmetry plane of the QL group velocity surface, and vice versa; however, the converse is not true for the QT modes of anisotropic media with symmetry lower than transverse isotropy. Depending on the direction, the QT slowness surface is concave, convex, or transitional between them. Some points of zero Gaussian curvature lying outside the symmetry planes of slowness surface may have their caustics mapping across the mirror symmetry plane, while others may map into a cusp on the symmetry plane of the corresponding group velocity surfaces, where Eqs. (13)–(17) for the QT mode are no longer valid.

For a zinc specimen the arrivals of QL and QT modes are easily identified, because a broadband signal is excited by a Heaviside step point source, whose temporal response is very well understood[17,28,32] and detected by the capacitive displacement sensor. The determination of elastic constants C_{11} and C_{13} is greatly facilitated by converting many group velocity data into the corresponding phase velocity data and then using Eqs. (6) and (7). When a piezoelectric detector is used, only the QL group velocity data are easily and accurately obtained, which can be converted into QL phase velocity data $V(\theta)$ through Eqs. (29)–(32). These phase velocity data may be fitted into Eq. (5) by using a more complicated nonlinear-least-squares method to obtain the three elastic constants C_{11}, C_{44}, and C_{13}. The nonlinear-least-squares method critically depends on the initial estimates of the elastic constants and its convergence is not always guaranteed. The determination of the elastic constants by the nonlinear-least-squares technique will be greatly facilitated if the value of either C_{11} or C_{44} or both are known by other methods, e.g., using either a surface skimming pseudo-L wave along the [100] direction on the top surface of a zinc specimen or the S mode plain wave traveling in the [001] direction. In the case of zinc, C_{33} can be determined with the QL group velocity data fitted into Eq. (32) and then using Eq. (33), and C_{44} is obtained with the PT group velocity along the [001] direction. The nonlinear-least-squares method applied to the QL phase velocity data of zinc yields C_{11}=163.7 GPa and C_{13}=52.4 GPa. All these values are listed in the no. 5 row of Table I and in excellent agreement with those of Ref. 27 in the same table. Similarly, with the knowledge of C_{33} as determined above and C_{11} identical to those of Ref. 27, one obtains C_{44}=40.0 GPa and C_{13}=49.3 GPa in fair agreement with the corresponding values of Ref. 27.

VI. CONCLUSIONS

Various novel techniques have been demonstrated that allow us to determine the elastic constants of an anisotropic solid from the measured group velocity data of elastic waves traveling along arbitrary directions in the symmetry plane within and without a cuspidal region. The first technique used for determination of mixed index elastic constants is entirely analytical, being based on the equations recently derived by one of the authors.[21] The usefulness of this analytical technique has been illustrated with the exemplary specimens of transversely isotropic zinc, cubic silicon, and orthotropic PEEK. The other techniques are indirect procedures, whereby the experimental group velocity data are first converted into the corresponding phase velocity data via polynomial expansions. In case that the phase velocity data $V(\theta)$ of both QL and QT modes are calculated for the set of the same angles θ, one can rely on the linear-least-squares optimization to accurately determine the relevant elastic constants. When only either of them is obtainable, we need to use the nonlinear-least-squares optimization procedure that fit the data into Eq. (5) for a similar purpose. The nonlinear-least-squares technique depends on the initial estimates of parameters and will be greatly facilitated if the number of the parameters to be determined by the technique is minimized. It is shown that all the elastic constants of zinc determined by the various methods compare very well with the corresponding elastic constants of Ref. 27, which were accurately determined.

ACKNOWLEDGMENTS

We deeply appreciate the financial support from the Office of Naval Research. Use of the facilities of the Materials Science Center (MSC) at Cornell University is also acknowledged. The MSC is funded from the National Science Foundation.

[1] M. J. P. Musgrave, *Crystal Acoustics* (Holden-Day, San Francisco, 1970).
[2] B. A. Auld, *Acoustic Fields and Waves in Solids*, 2nd ed. (Krieger, Malabar, FL, 1990).
[3] A. G. Every, Phys. Rev. B **22**, 1746 (1980).
[4] H. J. McSkimin, in *Physical Acoustics*, edited by W. P. Mason (Academic, New York, 1967), Vol. I, Part A, pp. 271–334.
[5] E. Schreiber, O. L. Anderson, and M. Soga, *Elastic Constants and Their Measurements* (Academic, New York, 1973).
[6] E. P. Papadakis, in *Physical Acoustics*, edited by W. P. Mason and R. N. Thurston (Academic, New York, 1967), Vol. 12, pp. 277–374.
[7] G. L. Peterson, B. B. Chick, C. M. Fortunko, and M. Hirao, Rev. Sci. Instrum. **65**, 192 (1994).
[8] I. Ohno, J. Phys. Earth **24**, 355 (1976).
[9] T. Goto and O. L. Anderson, Rev. Sci. Instrum. **59**, 1405 (1988).
[10] S. I. Rokhlin and W. Wang, J. Acoust. Soc. Am. **86**, 1876 (1989).
[11] S. K. Sahay, R. A. Kline, and R. Mignogna, Ultrasonics **30**, 373 (1992).
[12] B. Tang and E. G. Henneke, Nondestr. Testing Commun. **4**, 109 (1989).
[13] J. L. Rose, A. Pilarski, and Y. Huang, Res. Nondestr. Eval. **1**, 247 (1990).
[14] J. D. Aussel and J.-P. Monchalin, Ultrasonics **27**, 165 (1989).
[15] P. A. Doyle and C. M. Scala, in *Review of Progress in Quantitative Nondestructive Evaluation*, edited by D. O. Thompson and D. E. Chimenti (Plenum, New York, 1991), Vol. 10B, pp. 1453–1459.
[16] K. Y. Kim, W. Sachse, and A. G. Every, J. Acoust. Soc. Am. **93**, 1393 (1993).
[17] K. Y. Kim and W. Sachse, J. Appl. Phys. **75**, 1435 (1994).
[18] W. Sachse and K. Y. Kim, Ultrasonics **25**, 195 (1987).
[19] L. Niu, Ph.D. thesis, Cornell University, Ithaca, New York, 1992.
[20] A. G. Every and W. Sachse, Phys. Rev. B **42**, 8196 (1990).
[21] K. Y. Kim, Phys. Rev. B **49**, 3713 (1994).
[22] G. A. Northrop and J. P. Wolfe, in *Nonequilibrium Phonon Dynamics*, edited by W. E. Bron (Plenum, New York, 1985), pp. 165–242.
[23] A. G. Every, Phys. Rev. B **34**, 2852 (1986).
[24] M. Born and E. Wolf, *Principles of Optics*, 6th ed. (Pergamon, New York, 1980).
[25] F. R. Breckenridge, C. E. Tschiegg, and M. Greenspan, J. Acoust. Soc. Am. **57**, 626 (1975).
[26] K. Y. Kim, L. Niu, B. Castagnede, and W. Sachse, Rev. Sci. Instrum. **60**, 2785 (1989).
[27] K. Y. Kim and W. Sachse, Phys. Rev. B **47**, 10 993 (1993).
[28] A. G. Every and K. Y. Kim, J. Acoust. Soc. Am. **95**, 2505 (1994).
[29] K. Y. Kim, A. G. Every, and W. Sachse (unpublished).
[30] K. Y. Kim, T. Ohtani, A. R. Baker, and W. Sachse (unpublished).
[31] G. F. D. Duff, Philos. Trans. R. Soc. London Ser. A **252**, 249 (1960).
[32] R. G. Payron, *Elastic Wave Propagation in Transversely Isotropic Media* (Martinus Nijhoff, The Hague, 1983).